[AMERICAN JOURNAL OF SCIENCE, VOL. 276, APRIL, 1976, P. 425-454]

MINERAL REACTIONS IN PELITIC ROCKS: II. CALCULATION OF SOME P–T–X(Fe–Mg) PHASE RELATIONS

ALAN BRUCE THOMPSON

Department Geological Sciences, Hoffman Laboratory, Harvard University, Cambridge, Massachusetts 02138

ABSTRACT. On the basis of predicted phase relations in the system K_2O–FeO–MgO–Al_2O_3–SiO_2–H_2O, attempts have been made to calculate isobaric T–X(Fe–Mg) sections from available experimental and thermochemical data. T–X(Fe–Mg) relations, calculated at PH_2O = 5 kb, for reactions involving garnet–biotite–cordierite–sillimanite–quartz with muscovite or K-feldspar, are compared with available experimental data and compositions of coexisting phases from different metamorphic environments. Similarly, T–X(Fe–Mg) relations, calculated at PH_2O = 5 kb, for reactions involving garnet–biotite–staurolite–chlorite–cordierite–quartz–muscovite, are compared with experimental data and compositions of coexisting phases in a staurolite to sillimanite transition from west central Maine. These methods allow observed textural relationships between minerals, compositions of coexisting phases, experimental and thermochemical data to be assembled in a coherent framework. They may easily be extended to include other phases (minerals, melts, or fluids) or any other bulk rock composition.

INTRODUCTION

The schematics of displacements of three-phase triangles in the AKFM pelite projection in response to changing pressure, temperature, or aH_2O during metamorphism were discussed in part I. The compositional limits to the individual three-phase displacements were described by schematic isobaric T–X(Fe–Mg) and isothermal P–X(Fe–Mg) sections. In these sections, individual continuous reactions were represented by single divariant loops, and discontinuous reactions by the intersections of several continuous reaction loops.

It is possible to combine compositional data on AFM assemblages with available experimental and thermochemical data in an attempt to provide pressure-temperature calibration of continuous reactions. In order to do this, it is necessary to consider the thermodynamic basis for mineral facies in pelitic rocks. As outlined in part I, continuous (Fe–Mg) reactions may be thought of as the sum of the appropriate end-member reactions in the systems K_2O–MgO–Al_2O_3–SiO_2–H_2O (KMASH) and K_2O–FeO–Al_2O_3–SiO_2–H_2O (KFASH). Alternatively, continuous reactions may be thought as *either* end-member reaction (in KMASH *or* KFASH) plus the appropriate binary (Fe–Mg) exchange reaction.

THERMODYNAMIC BASIS FOR MINERAL FACIES IN PELITIC ROCKS

The chemical compositions and hence chemical potentials of the phases cordierite (*Crd*), chlorite (*Chl*), biotite (*Bio*), chloritoid (*Ctd*), staurolite (*Sta*), garnet (*Gar*), and aluminosilicate (*Als*) may be described by the components Al_2O_3–FeO–MgO with excess $KAl_3Si_3O_{10}(OH)_2$ (or $KAlSi_3O_8$), SiO_2, and H_2O. On the AFM projection from KAl_3O_5, SiO_2, and H_2O (J. B. Thompson, 1957), equal values of the chemical potential of the determining components are connected by "equipotential lines" (Korzhinskii, 1959, p. 85). The three minerals comprising a three-phase

AFM field have equal chemical potentials of the determining components. Similarly, two-phase AFM tie-lines are lines of equal chemical potentials of defining components. The importance of "thermodynamically valid" mineral projections and choice of components was discussed recently by Greenwood (1975).

In order that the compositional locations of three-phase fields and two-phase tie-lines (in the AFM projection) may be determined, it is necessary to understand how continuous reactions may be related to end-member equilibria (in KFASH and KMASH) through binary cation-exchange (Fe–Mg) equilibria.

Distribution coefficients and exchange potentials.—A consideration of the thermodynamic relations between a series of Fe–Mg crystalline solutions provides a useful example of the relations between exchange potentials and distribution coefficients (see also Kretz, 1961, 1972; Mueller, 1961; Albee, 1965a, p. 274-291).

Consider the end-member reactions between garnet, cordierite (anhydrous), sillimanite, and quartz (table 2 in pt. I; reaction 10)

$$3Fe_2Al_4Si_5O_{18} = 2Fe_3Al_2Si_3O_{12} + 4Al_2SiO_5 + 5SiO_2 \qquad (10)$$

$$3Mg_2Al_4Si_5O_{18} = 2Mg_3Al_2Si_3O_{12} + 4Al_2SiO_5 + 5SiO_2 \qquad (10')$$

for which at equilibrium we may write

$$2\mu[\text{Fe–Gar}] + 4\mu[\text{Sil}] + 5\mu[\text{Qtz}] = 3\mu[\text{Fe–Crd}] \qquad (i)$$

$$2\mu[\text{Mg–Gar}] + 4\mu[\text{Sil}] + 5\mu[\text{Qtz}] = 3\mu[\text{Mg–Crd}] \qquad (ii).$$

For each phase

$$\mu_i = \mu_i^\circ + nRT\ln a_i \qquad (iii),$$

and thus the equilibrium conditions may be written in terms of standard chemical potentials and activities. Thus, for (*i*) and (*ii*) at equilibrium with pure sillimanite and quartz (unit activity), we may write

$$2\mu^\circ[\text{Fe–Gar}] + 4\mu^\circ[\text{Sil}] + 5\mu^\circ[\text{Qtz}] - 3\mu^\circ[\text{Fe–Crd}] = -RT\ln [a_{\text{Fe-Gar}}^{\text{Gar}}]^2[a_{\text{Fe-Crd}}^{\text{Crd}}]^{-3} \qquad (iv)$$

and

$$2\mu^\circ[\text{Mg–Gar}] + 4\mu^\circ[\text{Sil}] + 5\mu^\circ[\text{Qtz}] - 3\mu^\circ[\text{Fe–Crd}] = -RT\ln [a_{\text{Mg-Gar}}^{\text{Gar}}]^2[a_{\text{Mg-Crd}}^{\text{Crd}}]^{-3}. \qquad (v)$$

For the case of pure end-member reactions (10) and (10′), the right-hand side (R.H.S.) of (*iv*) and (*v*) would be zero, because for pure phase the activity is unity ($a = 1$).

Subtracting (*v*) from (*iv*) we obtain,

$$2(\mu^\circ[\text{Fe–Gar}] - \mu^\circ[\text{Mg–Gar}]) - 3(\mu^\circ[\text{Fe–Crd}] - \mu^\circ[\text{Mg–Crd}] = -RT\ln[a_{\text{Fe-Gar}}^{\text{Gar}}]^2[a_{\text{Mg-Gar}}^{\text{Gar}}]^{-2}[a_{\text{Fe-Crd}}^{\text{Crd}}]^{-3}[a_{\text{Mg-Crd}}^{\text{Crd}}]^3 \qquad (vi).$$

If it is assumed that Fe–Mg garnet and cordierite crystalline solutions may be considered to be ideal ($\gamma = 1$), then because there are 3 equivalent

Fe–Mg sites in garnet, $[a_{Mg\text{-}Gar}{}^{Gar}]$ may be approximated by $(X_{Mg}{}^{Gar})^3$. Similarly for the two equivalent sites in cordierite $[a_{Mg\text{-}Crd}{}^{Crd}]$ may be approximated by $(X_{Mg}{}^{Crd})^2$. Activity models are presented in table 1, pt. I. With these substitutions (*vi*) becomes

$$2\mu^\circ[\text{Fe–Gar}] + 3\mu^\circ[\text{Mg–Crd}] - 2\mu^\circ[\text{Mg–Gar}] - 3\mu^\circ[\text{Fe–Crd}] =$$
$$-\text{RTln}\,(X_{Fe}{}^{Gar})^6(X_{Mg}{}^{Crd})^6(X_{Mg}{}^{Gar})^{-6}(X_{Fe}{}^{Crd})^{-6} =$$
$$-6\text{RTln}\,(X_{Fe/Mg}{}^{Gar})\,(X_{Mg/Fe}{}^{Crd}) \qquad (vii).$$

The quantity $(X_{Fe/Mg}{}^{Gar})\,(X_{Mg/Fe}{}^{Crd})$ is the *distribution coefficient* (identical to the equilibrium constant for an exchange reaction), and the quantity on the left-hand side (L.H.S.) of (*vii*) is the (Fe–Mg) *exchange potential* for the case of multicomponent ideal solutions. Additional components in natural phases (such as Mn) will be accounted for in the X terms (mol fractions in *vii*). However, this model becomes inadequate as the crystalline solutions deviate from ideality, as for example the case of extensive solution of Ca in garnet. Although the K_D involves ferrous iron, if the natural phase contains Fe^{3+} forming an ideal solution with Al, then the activity of almandine in natural garnet may be approximated by $(X_{Fe}{}^{X})^3(X_{Al}{}^{Y})^2$.

Exchange potentials from experimental data and natural assemblages.—The tie-lines representing two-phase fields on the AFM diagram are defined by the Fe–Mg exchange potential. These tie-lines are bounded by (define one side of) adjacent three-phase triangles. Therefore, distribution coefficients and hence exchange potentials may be determined from the compositions of phases in three-phase assemblages with different saturating phases. Relation (*vi*) will hold for *Gar–Crd* coexisting with *Als*, with *Bio*, or with hypersthene (*Hyp*) provided that the components remain the same. Ternary Al–Mg–Fe solution for *Chl* and *Bio* complicates the evaluation of Fe–Mg exchange potentials from different assemblages.

If the P–T locations of *both* (Fe and Mg) end-member reactions are known from experimental studies, it is possible to evaluate exchange potentials and their dependence upon pressure and temperature (see Thompson, 1974a, and below). The chemical potential difference between the *pure* phases defining an exchange reaction (called a *total exchange potential* by Thompson, 1974a) may be evaluated directly from Gibbs energy of formation data ($\Delta\overline{G}^\circ_f$), if known. In many cases it is necessary to estimate $\Delta\overline{G}^\circ_f$ for pure phases from phase-equilibrium studies (see Robie, 1965; Zen, 1973; Thompson, 1974b), where the precision of individual values of $\Delta\overline{G}^\circ_f$ is of the same magnitude as the total exchange potential.

Crude values of exchange potentials may be obtained from measured K_D values for coexisting minerals, where equilibration temperatures can be measured experimentally or estimated for natural assemblages. Care must be taken to obtain complete analyses of minerals that at least define local equilibrium. For example, a gravimetric analysis of a garnet obscures significant compositional variation due to growth zoning, dif-

fusion zoning, and the presence of inclusions. Complete microprobe analysis can at least provide a structural formula, and in some cases Fe^{3+} may be determined by recalculation.

Garnet–cordierite and garnet–biotite distribution coefficients from natural assemblages.—The compositions of adjacent garnet–cordierite and garnet–biotite pairs obtained from electron microprobe analyses were recalculated to end-member components and used to obtain values of $ln K_D$(Fe–Mg). Adjacent garnet–cordierite pairs from Union, Conn.; Sturbridge and Phillipston, Mass.; and Stoddard, N.H. show uniform core compositions but have retrograde-exchange rims (Hess, 1971; Richardson, ms; A. B. Thompson, unpub.). Approximate temperatures of equilibration (650° to 750°C) were estimated on the basis of mica–feldspar–Al_2SiO_5–quartz phase relations (Thompson, 1974a) corrected for Ca and reduced aH_2O where necessary. These temperatures were used in conjunction with *core* compositions of *Gar–Crd* to evaluate the temperature dependence of $ln K_D$(Fe–Mg) as shown by the solid-squares in figure 1A. Garnet–cordierite rim K_D's were calculated from the data of Osberg (1971) for assemblages from south-central Maine. An assumed equilibration temperature of 500°C for these minerals is consistent with independent temperature estimates in the interbedded calc–silicates (Ferry, 1976). In order to compensate for the probable error in estimation of temperature and the effect of other components on K_D, each data point (solid squares in fig. 1A) was fitted at ±50°C from the estimated value with ±5 percent for the calculated K_D value in the linear least squares analysis. These values may be compared with other published K_D values for different metamorphic grades (Chinner, 1962; Best and Weiss, 1964; Reinhardt, 1968; Okrusch, 1971; Hensen and Green, 1973; Dougan, 1974). Experimentally determined values of $ln K_D$(Fe–Mg) for garnet–cordierite obtained by Hensen and Green (1971, 1972) and by Currie (1971), together with their quoted estimates of precision of composition and temperature measurement, are shown by closed and open circles, respectively, in figure 1A.

Values of $ln K_D$(Fe–Mg) for garnet–biotite pairs were obtained using garnet–core and interior biotite compositions for samples from Union, Conn.; Sturbridge and Phillipston, Mass. (A. B. Thompson, unpub.; S. M. Richardson, ms). These values, with temperatures of about 700° and 650°C estimated above, are shown by solid squares in figure 1B. The data obtained by Guidotti (1974, estimated temperature near 600°C) for samples from west-central Maine and that obtained by Osberg (1971, estimated temperature near 500°C) were also used in the linear least squares analysis. These values may be compared with the data of Atherton (1968), Gorbatschev (1968), Saxena (1969), Lyons and Morse (1970), and Tracy (ms). The plot of $ln K_D$(Fe–Mg) between garnet and biotite and temperatures calibrated against O^{18}/O^{16} for quartz–magnetite, quartz–ilmenite, or quartz–garnet isotopic thermometers, obtained by Goldman and Albee (1976), gives temperatures about 50°C lower than that

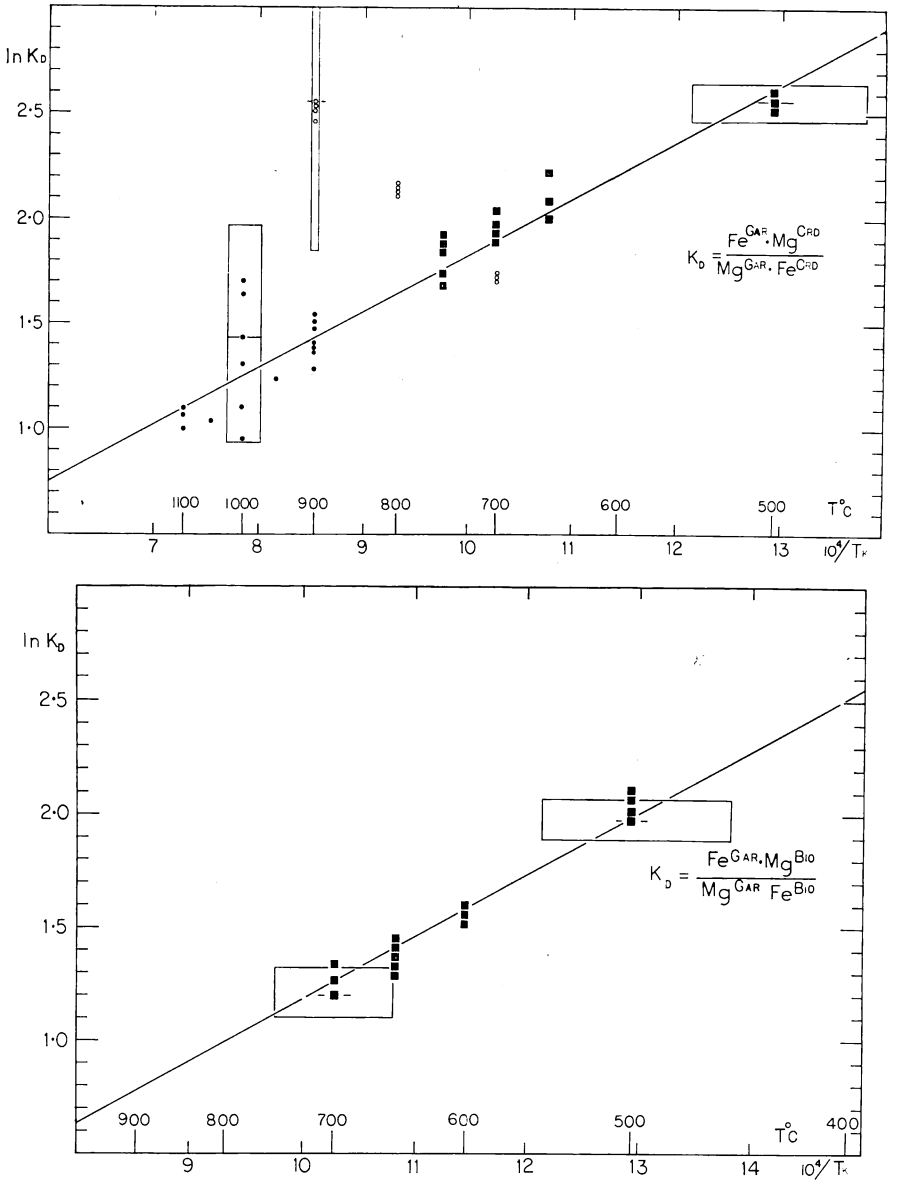

Fig. 1. Plots of $\ln K_D$ against $1/T_K$ for (Fe–Mg) exchange coexisting (A) *Gar–Crd* and (B) *Gar–Bio*. Values of $K_D = (Fe/Mg)_{Gar}$. $(Mg/Fe)_{Crd}$ were obtained from natural assemblages (solid squares) using the data of Osberg (1971, 500°C), S. M. Richardson (ms, 700°C) and A. B. Thompson (unpub., 650°, 700°, 750°C). Values of K_D $(Fe/Mg)_{Gar}$. $(Mg/Fe)_{Bio}$ were obtained from the data of Osberg (1971, 500°C), Guidotti (1974, 600°C), S. M. Richardson (ms, 700°C), and A. B. Thompson (unpub., 600°, 650°, 700°C). Temperature estimation and data fitting procedures are discussed in the text. (A) shows the experimental data of Hensen and Green (1971, 1972)—solid circles, and Currie (1971)—open circles, together with their quoted estimates of precision.

presented by figure 1B. Furthermore, values of $ln K_D$(Fe–Mg) determined for garnet–biotite pairs from high-grade metamorphic rocks show systematic displacements with increasing Ti in biotite.

While the temperature dependence of $ln K_D$(Fe–Mg) for *Gar–Crd* and *Gar–Bio* pairs as shown in figure 1 will be revised as more data become available and non-ideality of mixing is better understood, they may be used to provide crude two-phase exchange thermometers and for the determination of exchange potentials. Cation exchange reactions are particularly important in these regards, because they are virtually independent of pressure (see table 1) and independent of aH_2O.

Cation-exchange thermometers of this type may be calibrated against isotope exchange thermometers or other well calibrated cation exchange thermometers (for example, low manganese iron-titanium oxides) in natural assemblages. This type of information may be readily obtained from Mg/Fe^{2+} ratios commonly tabulated by workers during the comparison of mineral analyses (for example, Albee, 1972, p. 3255; Guidotti, 1974, p. 484). Mineral pairs with the largest Mg/Fe partition (for example, *Gar–Crd, Gar–Chl, Gar–Bio, Ctd–Chl,* and *Sta–Chl*) will be the most suitable for Fe–Mg cation-exchange thermometry, because they are present in a wide range of rock compositions and stable over a large range in metamorphic grade.

Continuous reactions and exchange potentials.—Values of $\Delta\bar{H}°/R$ and $\Delta\bar{S}°/R$ may be obtained from the PH_2O–T coordinates of end-member reactions if the stoichiometric coefficients, molar volume, and fH_2O are known. For a dehydration reaction the equilibrium condition ($\Delta\mu° = O$) may be represented by

$$\Delta\mu°/RT = \Delta\bar{H}°/RT - \Delta\bar{S}°/R + P\Delta\bar{V}°_s/RT + x\ln fH_2O \qquad (viii)$$

where x is the number of moles of H_2O. Thus a plot of ($x\ln fH_2O + \Delta\bar{V}°_s\ \Delta P/RT$) against $1/T_k$ (where $\Delta\bar{V}°_s$ is the volume change of pure solid phases, in cal bar^{-1}) will give a slope of $-\Delta\bar{H}°/R$ and intercept of $\Delta\bar{S}°/R$. Although the equation of state in the form of (viii) above assumes that $\Delta\bar{H}°$ and $\Delta\bar{S}°$ are independent of temperature (that is, ΔC_p is zero), this assumption is adequate for extrapolations over small ranges in temperature.

For the anhydrous reactions (10) and (10′), relation (iv) may be written to include analagous expression to (viii), that is

$$\begin{aligned}\Delta\mu°_{Fe}/RT &= -\ln(X_{Fe}^{Gar})^6(X_{Fe}^{Crd})^{-6} \\ &= \Delta H°_{Fe}/RT - \Delta\bar{S}°_{Fe}/R + P\Delta\bar{V}°_{Fe}/RT \end{aligned} \qquad (ix)$$

and

$$\begin{aligned}\Delta\mu°_{Mg}/RT &= -\ln(X_{Mg}^{Gar})^6(X_{Mg}^{Crd})^{-6} \\ &= \Delta H°_{Mg}/RT - \Delta\bar{S}°_{Mg}/R + P\Delta\bar{V}°_{Mg}/RT \end{aligned} \qquad (x)$$

TABLE 1

Thermochemical parameters for stoichiometric equations

Reaction (pt. 1, table 2)	End-member	$\Delta\bar{V}_s/R^*$ deg bar^{-1}	$\Delta\bar{S}/R^*$	$\Delta H/R^*$ deg	c	E	Reference
(1)	Mg–Mus–Kya	0.6846	3448.593	−2,753,016.078	−0.999	0.0057	1
(1)	Mg–Mus–Sil	−1.8629	24.219	−34,165.490	−0.999	0.0008	1
(7)	Mg–And	3.7590	378.041	−225,514.907	−0.997	0.7865	2
(10)	Fe–Sil	−1.9558	7.601	−13,994.579	−0.923	0.4738	3,4
(12)	Fe–Sil	0.2652	224.179	−164,300.445	−0.439	5.2676	3
(13)	Fe–Sil	1.3889	53.826	−30,835.457	−0.960	0.5945	3
(16)	Mg–Mus	2.0918	334.519	−199,049.040	−0.995	1.4742	1,5
Exchange reactions (values are per Fe–Mg exchangeable cation)							
	Gar–Bio	−0.0234	−1.560	+2,739.646	+0.976	−1.5605	Figure 1
	Gar–Crd	−0.0155	−0.896	+2,724.948	+0.968	−0.1037	Figure 1

End-member and exchange reactions have been fitted by least squares to the linear equation $Y = a + b/T$, where $a = \Delta\bar{S}/R$, $b = \Delta\bar{H}/R$. $Y = (x\ln f_{H_2O} + \Delta\bar{V}_s\Delta P/RT)$ for dehydration reactions, $(\Delta\bar{V}_s\Delta P/RT)$ for anhydrous reactions, and $(n\ln K_D + \Delta\bar{V}_s\Delta P/RT)$ for exchange reactions. The standard state for both solids and fluids is thus T, 1 atm.

The values of $\Delta\bar{S}/R$ and $\Delta\bar{H}/R$ are taken to three decimal places to avoid round-off error. The values of the correlation coefficient (c) and standard estimate of error (E) refer only to the precision of the data fitting and are no measure of their precision or accuracy.

The reference data sources are (1) Bird and Fawcett (1973), (2) Seifert and Schreyer (1970), (3) Richardson (1968), (4) Weisbrod (1973a), (5) Seifert (1970).

* The dimensionalities are a result of division of $\Delta\bar{V}_s$ in cal bar^{-1}, $\Delta\bar{S}$ in cal deg^{-1}gfw^{-1}, and $\Delta\bar{H}$ in cal gfw^{-1}, by R (1.98726 cal deg^{-1} gfw^{-1}).

Similarly, the exchange potential may be defined by subtracting (*x*) from (*ix*), compare (iv) − (v) = (vi) above, that is

$$\begin{aligned}\Delta\mu^{\circ}{}_{FeMg_{-1}}/RT &= (\Delta\bar{H}^{\circ}{}_{Fe} - \Delta\bar{H}^{\circ}{}_{Mg})/RT - (\Delta\bar{S}^{\circ}{}_{Fe} - \Delta\bar{S}^{\circ}{}_{Mg})/R \\ &\quad + P(\Delta\bar{V}^{\circ}{}_{Fe} - \Delta\bar{V}^{\circ}{}_{Mg})/RT \\ &= -61n\,(X_{Fe/Mg}{}^{Gar})(X_{Mg/Fe}{}^{Crd}) \\ &= -61nK_D(Fe\text{–}Mg) \qquad (xi).\end{aligned}$$

The divariant loops representing the continuous reactions may be constructed on isobaric (T–X) or isothermal (P–X) sections, if equations for two expressions of the type (*ix*), (*x*), or (*xi*) are available. These may be solved simultaneously (because $X_{Mg} = 1 - X_{Fe}$) to define the T–X and P–X loops (compare Thompson, 1974a, p. 176-187).

Evaluation of $\Delta\bar{H}^{\circ}/R$ and $\Delta\bar{S}^{\circ}/R$ for end-member and exchange reactions.—Values of $\Delta\bar{H}^{\circ}/R$ and $\Delta\bar{S}^{\circ}/R$ for several experimentally investigated reactions in the pure Fe- or Mg-systems were determined as slope and intercept values in a linear least squares analysis of data fitted as $(x\ln fH_2O + \Delta V^{\circ}{}_s\Delta P/RT)$ against $1/T_K$. Molar volume data for solid phases were taken from the compilation by Robie, Bethke, and Beardsley (1967), and fH_2O values were taken from the tabulation by Burnham, Holloway, and Davis (1969). The stoichiometric reaction coefficients presented in part I (table 2) were used, although they are usually different from those of the original authors. Values of $\Delta\bar{H}^{\circ}/R$, $\Delta\bar{S}^{\circ}/R$, and $\Delta\bar{V}^{\circ}/R$ are presented in table 1. The standard error and correlation coefficients refer only to the precision of data fitting and are no measure of accuracy.

The (Fe–Mg) data in figure 1 were used to evaluate $\Delta\bar{H}/R$ and $\Delta\bar{S}/R$ for the (Fe–Mg) exchange reactions between *Gar–Crd* and *Gar–Bio*. For these reactions using the formulae in part I (table 1), values of $n = 6$ for *Gar–Crd* and $n = 24$ for *Gar–Bio* are used in the conversion of $\ln K_D$ data to $\Delta\bar{H}/R$ and $\Delta\bar{S}/R$ values. Attempts were made to fit data for *Crd–Bio* (Fe–Mg) exchange, but the scatter of the calculated K_D values does not permit meaningful evaluation. This is a reflection of the similarity of $X_{Mg}{}^{Crd}$ and $X_{Mg}{}^{Bio}$. Values of $\Delta\bar{H}/R$ and $\Delta\bar{S}/R$ for (Fe–Mg) *Crd–Bio* exchange may be obtained from algebraic summation of the *Gar–Crd* and *Crd–Bio* data. Even though each calculated K_D was treated as four data points (±50°C and ±5 percent of K_D) the values of $\Delta\bar{H}/R$ and $\Delta\bar{S}/R$ carry considerable uncertainty. Crude limits may be placed on these values by comparison with estimated entropy data and enthalpy data evaluated from phase equilibrium studies and diffusion data (±2.5 cal $deg^{-1}mol^{-1}$ on $\Delta\bar{S}$ and ±1.0 kcal on ΔH, *per Fe–Mg*).

Although (Fe–Mg) exchange reactions are independent of aH_2O, the end-member and continuous reaction coefficients for cordierite reactions (pt.I, table 2) may be seriously in error, because water may be an essential part of the cordierite structure (see Stout, 1975 and references therein). The entropy contribution of H_2O (and Al/Si disorder) will significantly affect the Gibbs energy values and stability (see Hess, 1969, p. 196; Newton, 1972; Chernosky, 1974). The fact that the present values were

calculated from experimental studies and natural assemblages as opposed to fundamental thermochemical data may lessen the uncertainty. The consequences of the present assumptions will be realized when additional data become available.

End-member P–T grids and continuous reactions.—In the absence of precise data for the P–T locations of most of the end-member reactions in KFASH and KMASH and of the appropriate thermochemical data, these quantities must be estimated or deduced by extrapolation. Several workers have constructed partial PH_2O–T grids for KFASH (Hoschek, 1969; Ganguly, 1968, 1972; Fed'kin, 1972; Froese, 1973) and for KMASH (Schreyer and Seifert, 1969). As noted above, the continuous and discontinuous reactions in KFMASH originate and terminate at the univariant lines and invariant points respectively for the KFASH and KMASH systems (for a specific aH_2O and values of fO_2 such that the relevant phases are stable). These calculated grids for end-member systems utilize measured molar volume data and tabulated or estimated entropy data for calculation of dP/dT. The locations of the end-member reactions (which are constrained by the exchange potentials) and the $\Delta\bar{V}°$ and $\Delta\bar{S}°$ data may be used to calculate P–X and T–X loops for continuous reactions. The assumption of ideal (Fe–Mg) crystalline solution simplifies the calculation (compare relations *ix* and *x*).

Several P–X and T–X diagrams have been calculated from available experimental studies and estimated thermochemical data to illustrate the relationships between observations of natural assemblages and the predicted phase relations, as described in the following section.

COMPARISON OF PREDICTED RELATIONS WITH EXPERIMENTAL DATA AND NATURAL ASSEMBLAGES

The usefulness and accuracy of the calculated P–T–X coordinates for continuous and discontinuous reactions can be tested against assemblages where the compositions of coexisting phases, P, T, aH_2O, and fO_2, are known with some degree of accuracy.

Some experimental studies have included measurement of the compositions of coexisting Fe–Mg crystalline solutions at known P, T (Hensen and Green, 1971, 1972), but equilibrium may not have been achieved. Other studies may reflect equilibrium conditions, but report only approximate compositions (Hirschberg and Winkler, 1968), or fail to report compositions of coexisting phases (Hoschek, 1969), such that the divariant reactions cannot be defined in terms of P–T–X. In these latter studies only one boundary of a divariant loop for a particular Fe/Mg composition is reported.

In spite of these problems, calculated P–T, P–X, and T–X sections for reactions involving *Gar–Bio–Crd–Als–Mus–Ksp–Qtz–H_2O* and for *Sta–Bio–Crd–Chl–Gar–Als–Mus–Qtz–H_2O* may be compared with available experimental data and compositions of coexisting phases in natural assemblages.

REACTIONS INVOLVING GARNET–BIOTITE–CORDIERITE–Al_2SiO_5–QUARTZ WITH MUSCOVITE OR K-FELDSPAR

Garnet–cordierite–sillimanite–quartz equilibria. — A considerable amount of recent discussion has been concerned with Fe–Mg reactions involving *Gar–Crd–Als–Qtz*. The plot of $\ln K_D$ against 1/T for Fe–Mg exchange between *Gar–Crd* (fig. 1) supports the trend of the data of Hensen and Green (1971, closed circles) and is in disagreement with that of Currie (1971, 1974, open circles). The negative dP/dT for the Fe end-member reaction (10) as experimentally determined by Richardson (1968) and Weisbrod (1973a) is supported by the negative slope obtained for the analagous reaction in the pure Mn system by Dasgupta, Seifert, and Schreyer (1974). Although the pure Mg-end member reaction is metastable, indirect evidence apparently implies a positive dP/dT (Newton, 1972; Newton, Charlu, and Kleppa, 1974; Hutcheon, Froese, and Gordon, 1974). The extent to which the actual slope is modified by Al–Si ordering in *Crd* and *Sil*, the H_2O content of *Crd*, or the *Kya-Sil* reaction is not known. Although the present study considers anhydrous cordierite, the experimental data of Newton (1972) and Green and Vernon (1974) indicate that $X_{H_2O}^{Crd}$ and hence the stability field of cordierite depend upon fH_2O.

The values of $\Delta\bar{H}°_{Fe}/R$ and $\Delta\bar{S}°_{Fe}/R$ (in table 1) obtained from the data of Richardson (1968) and Weisbrod (1973a) for the Fe-reaction 10 (*Crd* = *Gar* + *Sil* + *Qtz*) were combined with those evaluated for the (Fe–Mg) exchange potential (fig. 1A, table 1) to obtain an equation of state for the Mg-reaction, that is,

$$\Delta\mu°_{Mg}/RT = 30344.27/T_K - 12.982 - 1.909P/T_K.$$

This equation generates the negative P–T slope shown in figure 2B, which will be metastable in the pure Mg system (see Hensen and Green, 1971; Kleppa and Newton, in press).

Isothermal P–X loops have been calculated (fig. 2A) from the above locations of end-member reactions, and their molar volume changes through simultaneous solution of the equations,

$$ln X_{Fe}^{Gar}/X_{Fe}^{Crd} = \Delta\bar{V}°_{Fe}(P_{Fe}–P)/6RT$$

and

$$ln X_{Mg}^{Gar}/X_{Mg}^{Crd} = \Delta\bar{V}°_{Mg}(P_{Mg}–P)/6RT$$

The loops (fig. 2A) indicate lower values of P_{Mg} than implied by the 900° and 1000°C data of Hensen and Green (1971, p. 328), and consequently the calculated (P–X) loops fall some 3 kb below their data. The 700° and 900°C results of Currie (1971) are also shown in figure 2A, together with the estimated errors of composition. The calculated P–X loops in figure 2A imply that *Crd* should not be stable with *Gar* + *Sil* + *Qtz* in the 900° and 1000°C data of Hensen and Green (1971). This conclusion is not easily reconciled with the apparent reversibility of *Gar–Crd* compositions on the P–X loop at 1000°C and 9 kb (Hensen, 1973), despite the fact

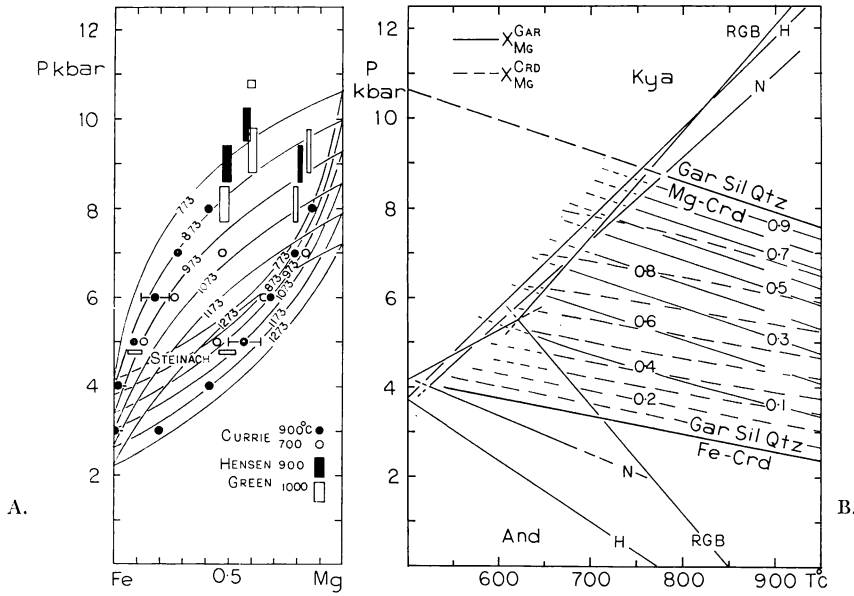

Fig. 2 (A). Comparison of calculated (solid lines) and experimentally determined isothermal P–X(Fe–Mg) sections (*degrees kelvin*) for the reaction 3Crd ⟶ 2Gar + 2Sil + 5Qtz. Experimental data of Hensen and Green, 1971; Hensen, 1973 shown by closed boxes for 900°C and open boxes for 1000°C. The open square at 1000°C, 10.8 kb (Hensen and Green, 1972, p. 351) shows their data for the *Gar* composition with trace of *Crd*, in the Ca–Na–free system. The data of Currie (1971) is shown by closed circles for 900°C and open circles for 700°C, the horizontal bars (*Gar* 6 kb, 900°C; *Crd* 5 kb, 900°C) indicate Currie's estimates of compositional accuracy. The ranges of *Gar–Crd* compositions from the *Steinach* aureole (Okrusch, 1971, with *Bio* and *Sil, Qtz, Ksp*) are shown by open horizontal rectangles near 5 kb.

B. P–T diagram with X_{Mg}^{Gar} (solid lines, odd numbers) and X_{Mg}^{Crd} (dashed lines, even numbers) contours for the divariant (Fe–Mg) reaction, compare Hensen and Green (1973, p. 154). The Mg-reaction will not be stable due to the appearance of hypersthene. The Al_2SiO_5 phase relations from Newton (1966, *N*), Richardson, Gilbert, and Bell (1969, *RGB*), and Holdaway (1971, *H*) are shown. Melting relations and other stable equilibria have been omitted.

that the phases show extensive compositional zoning. Experimental difficulties, which could influence pressures of cordierite breakdown reactions, have been discussed by Newton (1972) and Newton, Charlu, and Kleppa (1974, p. 296). The present results are comparable with those calculated by Hutcheon, Froese, and Gordon (1974) despite the differences in sign of dP/dT. Although the values of $\Delta\bar{H}/R$ and $\Delta\bar{S}/R$ obtained from the $\ln K_D$ data in figure 1 are certainly approximate, both sets of experimental data are incompatible with molar volume data. The hexagonal cordierite values tabulated by Robie, Bethke, and Beardsley (1967, p. 65) were used because the data for orthorhombic Fe- and Mg–cordierite does not appear to be consistent. The calculated (P–X) loops do not change significantly using Hsu's (1968) volume data for Fe–cordierite (1574.1Å^3 = 5.664 cal bar^{-1}).

The same data have been used to calibrate X_{Mg} (*Gar* and *Crd*) isopleths in equilibrium with *Sil–Qtz* on a P–T diagram (fig. 2B). This diagram is of the same form as that of Hensen and Green (1973, p. 154) but refers to the $MgO–FeO–Al_2O_3–SiO_2$ system. These workers note (1972, p. 351) that the *Gar–Crd–Sil–Qtz* reaction will be displaced to lower pressures with $CaO–Na_2O–K_2O$ impurities.

Garnet–biotite–cordierite–sillimanite–quartz equilibria in natural assemblages.—The coexisting phases in the hornfelses of the Steinach aureole in Bavaria have been analyzed with a microprobe by Okrusch (1971). He estimates (p. 17) that the transition from low to high grade took place close to the *And–Sil* reaction and the breakdown of *Mus–Qtz*, suggesting PH_2O in the range 3 to 4 kb and temperatures greater than 640° to 680°C. Hensen and Green (1973, p. 160) suggests pressures near 6.6 kb and temperatures near 690°C. Use of the $\ln K_D$-1/T plots in figure 1 gave temperatures between 700° and 650°C for *Gar–Crd* and *Gar–Bio* pairs. The isopleths in figures 2A and B suggest pressures near 4.8 kb for K_D determined from Okrusch's data, relative to the Fe–Mg system. However, the garnets in the aureole contain between 5.5 and 13 mol percent spessartine and about 3 mol percent "grandite." According to the data of Weisbrod (1973b) the amount of Mn could lower the equilibration pressure by 0.4 to 0.8 kb.

Compositions of coexisting phases in high grade pelitic gneisses from the northwest Guayana Shield, Venezuela were determined by Dougan (1974) using X-ray fluorescence, atomic absorption, and chemical techniques. He (p. 180-182) used the Hensen-Green (1973) and Currie (1971) methods of (Fe–Mg) cation thermometry for *Gar–Crd* to obtain metamorphic temperatures. The former data give temperatures too high (815°-820°C) and the latter too low (645°-665°C) by comparison with Fe–Ti oxide thermometry (700°-800°C) and the absence of muscovite in migmatites. The $\ln K_D$ data in figure 1 gave temperatures of 760° to 825°C for *Gar–Crd* and 750° to 800°C for *Gar–Bio*.

Calibration of garnet–biotite–cordierite–sillimanite–quartz relations with muscovite or K-feldspar.—The compositional variation of the assemblages *Gar–Bio–Sil* and *Bio–Crd–Sil* (both with *Ksp–Qtz*) with increasing grade (Dougan, 1974, p. 174) support those predicted in part I (fig. 3B). An attempt has been made to calibrate the P–T–X(Fe–Mg) locations of the continuous reactions involving *Gar–Bio–Crd–Sil–Qtz* with either *Mus* or *Ksp*. The locations of some of the Mg and Fe end-member reactions, together with other relevant equilibria, are shown in figure 3.

The Mg-reaction 3 (Mus + Crd = Bio + Sil + Qtz) was constructed from the experimental data of Seifert (1970) and Bird and Fawcett (1973) with dP/dT of −10 bar deg^{-1}. This reaction intersects the K-Mus + Qtz = Ksp + Sil + H_2O reaction of Chatterjee and Johannes (1974) at 710°C, 5.7 kb leading to the Mg-reaction (Bio + Sil + Qtz = Ksp + Crd + H_2O) with a calculated dP/dT of +10 bar-deg^{-1}. The location

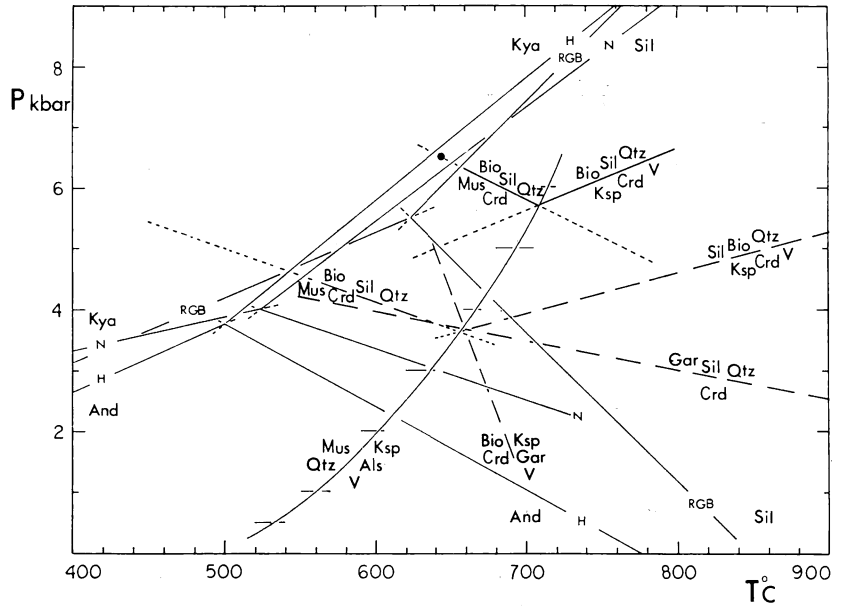

Fig. 3. P_{H_2O}–T diagram showing the Mg end-member reactions (solid lines) involving *Bio–Sil–Crd–Qtz* with *Mus* or *Ksp* (after Seifert, 1970) and the inflection at the Mus + Qtz = Ksp + Als + H_2O reaction (Chatterjee and Johannes, 1974). The calculated locations of the Fe-reactions (see text) are shown (dashed lines) relative to the Fe-reaction Crd = Gar + Sil + Qtz and the Mus + Qtz = Ksp + Als + H_2O reaction.

of reactions in the pure Fe-system was determined using estimated entropy data and tabulated volume data to obtain dP/dT.

The estimated entropy values used in determining dP/dT were obtained by two methods. The first method utilized the "oxide summation method" of Latimer (1951) and Fyfe, Turner, and Verhoogen (1958, p. 26-27, 116) with the appropriate corrections for actual versus *oxide-sum* molar volumes. The entropy values obtained at 25°C were extrapolated for calculations in the 600° to 700°C range (see values in table 2). The second method utilized the "entropy of dehydration" plus "entropy change of alumina coordination" method of Albee (1965b; 1972, p. 3261) and Hess (1969, p. 193). The H_2O and alumina values presented by Hess were used in a comparison of both methods, and the results are presented in table 2.

The location of the Fe end-member curve in figure 3 was obtained from the dP/dT data in table 2 plus additional constraints from available experimental data and a multisystems analysis of the appropriate equilibria (fig. 4). The extrapolated intersection of the Fe reaction (10, Crd = Gar + Sil + Qtz) with K-Mus + Qtz = Ksp + Sil + H_2O (fig. 3) gives a crude P–T location of the Fe-multisystem (fig. 4). An additional constraint is the location of the Fe reaction (17, Bio + Crd + Qtz = Gar

TABLE 2

Estimated dP/dT for some Fe end-member reactions

Reactions involving three-AFM phases, with Mus or Ksp (pt. I, table 2)		dP/dT bars deg^{-1} Method (1)	Method (2)
(17)	4Bio* + 21Qtz + 5Crd = 14Gar + 12Ksp + 12H_2O	−53	−41
(17)	2Bio + 7Crd = 10Gar + 6Mus + 3Qtz	−1	+2
(3)	Bio + 7Sil + 14Qtz = 4Crd + 3Ksp + 3H_2O	+10	+6
(3)	4Crd + 3Mus = Bio + 10Sil + 11Qtz	−9	−5
(2)	8Gar + 9Mus = 3Bio + 14Sil + 13Qtz	+8	+9
(2)	3Bio + 5Sil + 22Qtz = 8Gar + 9Ksp + 9H_2O	+62	+54
Reactions involving two-AFM phases, with Mus and Ksp			
	2Gar + 4Mus + 9Qtz = 3Crd + 4Ksp + 4H_2O	+8	+10
	3Bio + 5Mus + 27Qtz = 8Gar + 14Ksp + 14H_2O	+33	+34
	Bio + 7Mus + 21Qtz = 4Crd + 10Ksp + 10H_2O	+13	+14

Method 1 uses estimated Third-Law entropies (tabulated plus *oxide-summation method*) to calculate dP/dT. The following values (in the 600°-700°C) range were used: Gar = 198, Bio* = 681, Crd = 259, Sil = 68.6, Mus = 188, Ksp = 130, Qtz = 26.8, H_2O = 36.5, in cal deg^{-1} gfw^{-1}.

Method (2) uses an entropy of dehydration value of 14 cal gfw-H_2O^{-1} and a value of $Al^{VI} \rightarrow Al^{IV}$ of 2.39 cal Al^{-1} (see Albee, 1965a, p. 516; 1972, p. 3261; Hess, 1969, p. 193).

In both cases molar volumes (for 298°K, 1 atm) were obtained from Robie, Bethke, and Beardsley (1967) and a value of $\bar{V}_{H_2O}$ = 33.9 cm^3 was used (660°C, 2 kb data of Burnham, Holloway, and Davis, 1969, p. 21). Thus at higher pressures the dehydration reactions should have greater values of dP/dT.

* Biotite formula as in table 1, pt. I.

+ Ksp + H_2O) determined by Rutherford and Eugster (1967 at 665° ± 5°C at PH_2O = 2 kb with fO_2 buffered by graphite–methane–H_2O. For the same PH_2O, a temperature of 685°C was obtained for fO_2 buffered by quartz–fayallite–magnetite (M. Rutherford, personal commun., 1975).

The P–T locations of the Mg and Fe end-members for reactions (3, Mus + Crd = Bio + Sil + Qtz and Bio + Sil + Qtz = Crd + Ksp + H_2O) allow calculation of isothermal P–X(Fe–Mg) and isobaric T–X (Fe–Mg) sections, using estimated or measured $\Delta\bar{V}°$ or $\Delta\bar{S}°$ for end-member reactions (fig. 5). The discontinuous reactions (XVII) involving *Bio–Gar–Crd–Sil–Qtz* (with *Mus* or *Ksp*) were located by the intersections of the *Crd–Bio–Sil* (3) loops with the *Gar–Crd–Sil* (10) loop (with *Qtz, Mus,* or *Ksp* as appropriate). The unique values of X_{Mg} for *Gar–Bio–Crd* at these discontinuous reactions permitted approximate location of the *Gar–Bio–Sil* (2) loops (with *Qtz, Mus,* or *Ksp*) relative to the values of T_{Fe} as obtained from the data in table 2 and figure 4. The temperatures of the discontinuous reactions (XVII) involving *Bio–Gar–Crd–Sil–Qtz* (with *Mus* or *Ksp*) at PH_2O = 5 kb (fig. 5) may be compared with those calculated by Hess (1969, p. 197; 1973). The discontinuous reaction with *Mus* lies at higher temperature and that with *Ksp* at lower temperatures than the data of Hess. Only continuous reactions involving *Sil* are shown in figure 5, but reactions (17) involving *Gar–Bio–Crd* (without *Sil*) also originate at the appropriate discontinuous reactions. The representation

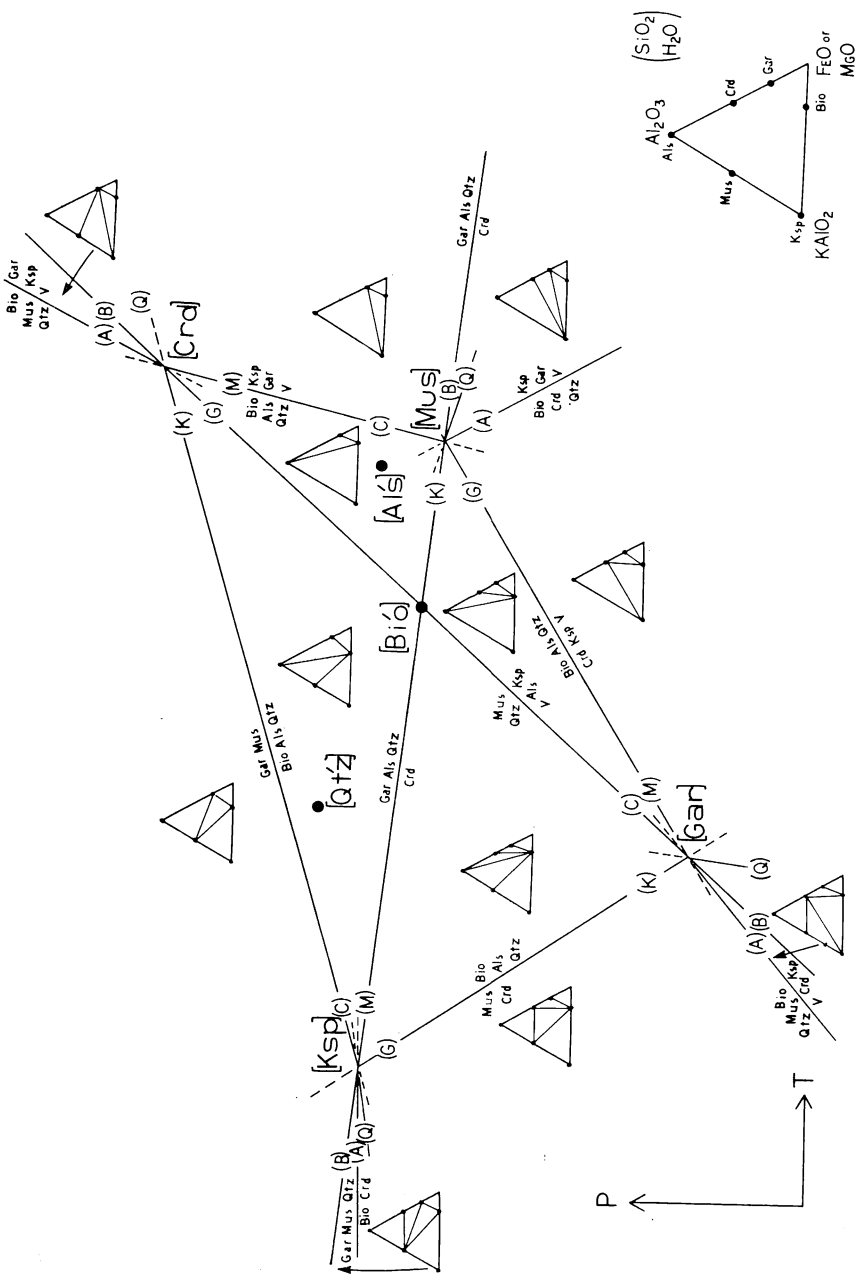

Fig. 4. Schematic P_{H_2O}–T diagram for reactions involving *Gar–Bio–Crd–Als–Qtz–Mus–Ksp* for either KFASH or KMASH systems. The estimated values for dP/dT (KFASH) are presented in table 2. The effects of phengite substitution in *Mus* will modify the phase relations as discussed by Tracy (ms). Metastable invariant points are indicated by primed phase absent.

of these types of equilibria on P–X (Fe–Mg) diagrams has been discussed by Hensen (1971, p. 200-203) and may be located on figure 5 using Rutherford and Eugster's (1967) data for the Fe-reaction (17) involving *Bio* + *Crd* + *Qtz* = *Gar* + *Ksp*. Needless to say the location of reactions in figures 3 and 5 will require modification when suitable data become available. In natural assemblages the continuous reactions leading to the discontinuous reaction (XVII, *Bio* + *Sil* + *Qtz* → *Gar* + *Crd* + *Ksp*) will be involved with an anatectic melt phase if $P_{total} \approx P_{H_2O}$.

Comparison of calculated and observed T–X(Fe–Mg) relations for garnet–biotite–cordierite–sillimanite–quartz equilibria.—A T–X(Fe–Mg)

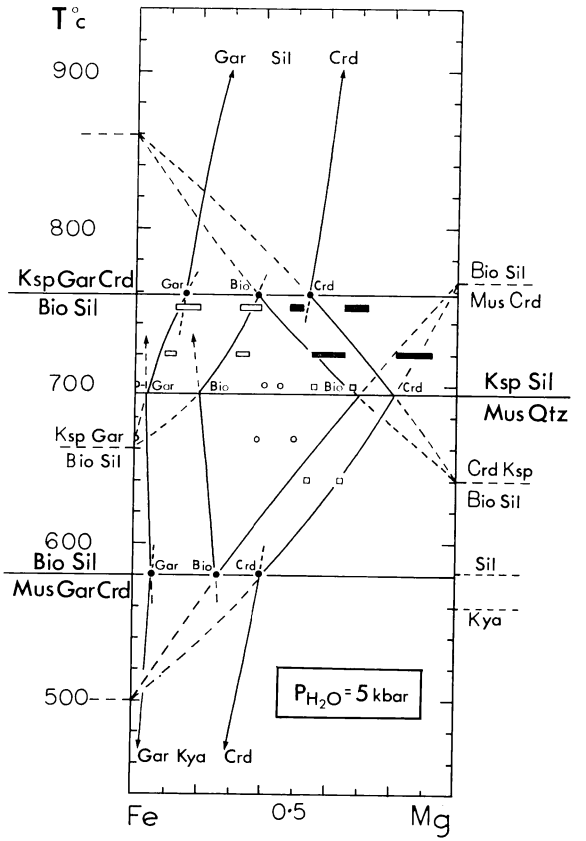

Fig. 5. Calculated T–X(Fe–Mg) section, P_{H_2O} = 5 kb, for the continuous and discontinuous reactions involving Gar–Bio–Crd–Als–Qtz (Mus or Ksp), see part I, figure 3. The location of the Gar–Crd–Als–Qtz reaction is taken from figure 2. The end-member temperatures for continuous reactions are taken from figure 3. The horizontal rectangles at 720° and 750°C show the ranges of *Gar–Bio–Sil* (open) and *Bio–Crd–Sil* (solid) from Dougan (1974). Compositions of coexisting *Bio–Crd* (with *Sil, Mus, Qtz*) shown as open squares and coexisting *Gar–Bio–Crd* (with *Sil, Mus, Qtz*) shown as open circles are taken from the experimental results of Hirschberg and Winkler (1968). The inflections at Al_2SiO_5 boundaries are not shown.

section for $P_{total} = P_{H_2O} = 5$ kb is shown in figure 5. The phase relations illustrated by Dougan (1974, p. 174) correspond to conditions below the discontinuous reaction (XVII, Bio + Sil = Gar + Crd + Ksp). The compositional ranges of coexisting phases from his study are located approximately on the calculated T–X(Fe–Mg) section in figure 5 (open rectangles, *Gar–Bio–Sil*; closed rectangles, *Crd–Bio–Sil*). The fact that the natural *Crd–Bio* (+*Sil*) compositions are more magnesian than calculated may indicate that continuous reaction (3, Bio + Sil + Qtz → Crd + Ksp + H_2O) is incorrectly located or that the natural assemblages probably equilibrated at higher pressure (5 to 7 kb, see fig. 3). With increasing pressure the calculated temperatures increase for the discontinuous reaction (XVII) and the continuous reaction (3), both involving *Ksp–Qtz*, and the phases involved have relatively higher values of X_{Mg}.

Hirschberg and Winkler (1968) reported experiments upon natural compositions of *Chl* + *Mus* + *Qtz* for two different chlorites (X_{Mg} = 0.2 and 0.6). Although they did not buffer fO_2 and hence the bulk MgO/FeO ratio may not represent the initial composition if magnetite or hematite formed, their data suggest that the association *Crd–Bio–Sil–Mus–Qtz* becomes more Mg-rich with increasing P and T. The compositions of coexisting *Crd* and *Bio* (with *Mus–Sil–Qtz*) at 640°C, 5 kb (X_{Mg}^{Crd} = 0.64, X_{Mg}^{Bio} = 0.53) may lie on the continuous reaction loop *Crd–Bio–Sil–Mus–Qtz* (open squares in fig. 5). The natural samples used in their experiments contained impure *Mus*, and thus their data at 700°C, 5 kb (X_{Mg}^{Bio} = 0.56; X_{Mg}^{Crd} = 0.68) may lie on the continuous reaction loop *Crd–Bio–Sil–Ksp–Qtz* (see Hirschberg and Winkler, 1968, p. 35, table 6). Their results on the X_{Mg} = 0.2 composition of *Chl* + *Mus* + *Qtz* (p. 28, table 4) at 666° and 700°C at 5 kb are shown in figure 5 by open circles. These data representing the association *Gar–Bio–Crd* with *Sil* do not correspond to any of the calculated continuous reactions.

The 5 kb isobaric T–X (Fe–Mg) section in figure 5 shows the predicted change of T_{Mg}:T_{Fe} (see pt. I) for the continuous reactions 3 (involving *Crd* + *Bio* + *Sil* + *Qtz* with either *Mus* or *Ksp*) and 2 (involving *Gar* + *Bio* + *Sil* + *Qtz* with either *Mus* or *Ksp*). The predicted displacements for the continuous reactions (2) and (3) involving *Ksp* are supported by the observations of Dougan (1974). Since the continuous reactions (2) and (3) with *Mus* + *Qtz* do not involve dehydration (see pt. I, table 2) their predicted displacements are based upon dP/dT calculated from entropy and volume data. The compositions of coexisting *Gar–Bio–Sil–Mus–Qtz* determined by Tracy (ms) in metapelite samples from central Massachusetts indicate that observed displacements of *Gar–Bio–Sil* cannot be assumed to be the result of changing temperature only. The steep T–X(Fe–Mg) loop (fig. 5) for the continuous reaction (2, Mus + Gar → Bio + Sil + Qtz) and the small dP/dT for the end-member reaction (table 2) suggest that changing pressure would have much larger effects on compositions of phases than changing temperature.

The locations of the discontinuous reactions involving *Gar–Bio–Crd–Sil–Qtz,* with *Mus* or *Ksp,* are determined from the intersections of the continuous reactions (2) and (3), with *Mus* or *Ksp,* with the calculated P–T–X (Fe–Mg) location of the continuous reaction 10 (*Crd* = *Gar* + *Sil* + *Qtz*). If the P–X (Fe–Mg) data of Hensen and Green (1971) had been used for reaction (10), then the discontinuous reaction (XVII, Bio + Sil = Ksp + Gar + Crd) would occur at higher temperatures, and the reaction (XVII, Mus + Gar + Crd = Bil + Sil) would occur at lower temperatures than shown in figure 5. In both cases, the phases involved would have higher X_{Fe} than those shown. With increasing pressure the discontinuous reaction (XVII, involving *Ksp*) moves to higher temperatures, and that with *Mus* moves to lower temperatures. For both cases, the composition of phases involved at higher pressures become richer in X_{Mg} relative to those shown in figure 5 for $PH_2O = P_{total} = 5$ kb.

The calculated phase relations in figures 3 and 5 do not include the presence of a silicate melt phase. At $PH_2O = 5$ kb melting would occur above the *K-Mus* + *Qtz* reaction at about 730°C and in natural assemblages containing sodic muscovite and albitic feldspar would occur near 640°C (for $PH_2O = P_{total}$, Thompson, 1974a, fig. 10). Obviously for $aH_2O < 1$, the dehydration reactions would occur at lower temperatures, and initial melting would begin at higher temperatures. The K_D(Fe–Mg) would still hold for pairs of phases in equilibrium with an anatectic melt, but the nature of the continuous reactions would change. The greater solubility of Fe than Mg in anatectic melts formed from pelitic rocks would displace the continuous reactions accordingly. Experimental determination of the continuous reactions for the case $PH_2O = P_{total}$ at temperatures in the melting region will not reproduce the continuous reactions illustrated in figure 5.

TRANSITION FROM STAUROLITE TO SILLIMANITE ZONE, WESTERN MAINE

The work of Guidotti (1970, 1974) and Guidotti, Cheney, and Conatore (1975) provides compositional data for complete AFM facies types in a staurolite to sillimanite zone facies series from adjacent quadrangles in Western Maine. The facies types show the discontinuities (XVIII) *Sta* + *Chl* + *Mus* → *Bio* + *Sil,* possibly (VIII) *Chl* + *Mus* → *Bio* + *Crd* + *Sil,* and at higher grade (VII) *Sta* + *Mus* → *Gar* + *Bio* + *Sil.* Guidotti (1974, p. 489) suggests pressures near 4 kb (below the Al_2SiO_5 triple point) and temperatures in the range 570° to 670°C, with aH_2O in the range 0.8 to 0.9 for the metamorphism (see Guidotti, 1970, p. 325). The continuous reactions leading to these discontinuities are shown schematically in pt I (figs. 1 and 2).

The compositional ranges of coexisting *Sta–Bio* (with *Sil, Mus, Qtz*) determined by Guidotti (1970) are shown by open rectangles at 650°C on the T–X(Fe–Mg) diagram in figure 6. Guidotti (1974) presents data on the compositions of phases involved in continuous reactions leading to the discontinuous reaction (XVIII, Sta + Chl + Mus → Bio + Als +

Qtz + H_2O). The compositional ranges are shown by the solid rectangles at 610°C on the T–X(Fe–Mg) diagram in figure 6. Guidotti, Cheney, and Conatore (1975) present data on the compositions of coexisting *Chl–Crd–Bio* occurring in pyrrhotite-rich pelites, where the extremely siderophile sulphide results in the formation of extremely magnesian silicates. This assemblage suggests that the discontinuous reaction (VIII, *Chl* + *Mus* → *Bio* + *Crd* + *Als*) was not reached at this grade. The maximum X_{Fe} observed for these phases is shown by the vertical arrows in figure 6.

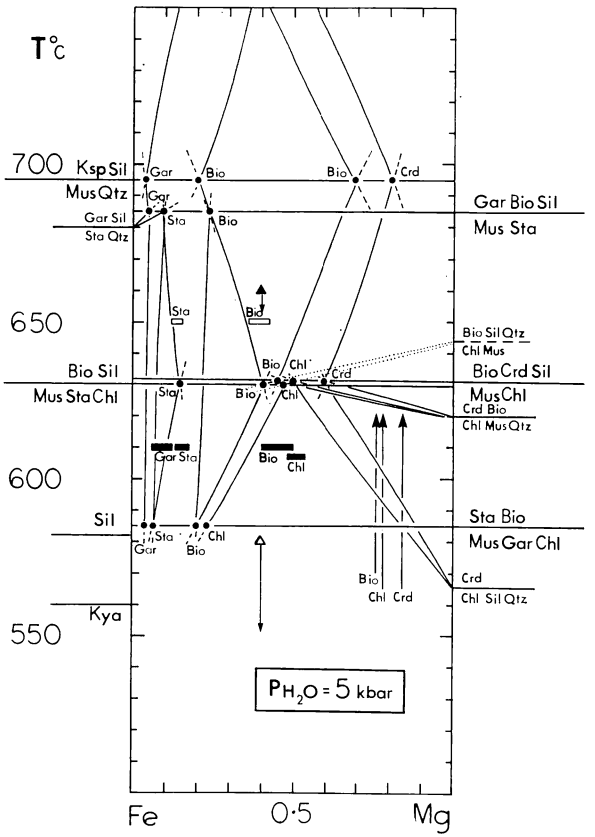

Fig. 6. Calculated T–X(Fe–Mg) section, P_{H_2O} = 5 kb for the continuous and discontinuous reactions shown in part I, figure 2. The Bio–Crd–Sil and Gar–Bio–Sil data are taken from figure 5, and other end-member reactions are discussed in the text. The highest values of X_{Fe} for *Bio–Chl–Crd* from Guidotti, Cheney, and Conatore (1975) are shown by vertical arrows. The range of compositions of coexisting *Gar–Sta–Bio–Chl* (Guidotti, 1974) are shown by solid horizontal bars. The ranges of compositions of coexisting *Sta–Bio–Sil* (Guidotti, 1970) are shown by open horizontal bars. The solid and open triangles show the data of Hoschek (1969; X_{Fe} = 0.6) for the divariant reactions 5 (Sta + Mus → Bio + Sil) and 22 (Chl + Mus → Sta — Bio), respectively. The constraints on the locations of continuous and discontinuous reactions are discussed in the text.

Calibration of staurolite–biotite–garnet–sillimanite–chlorite–cordierite–muscovite–quartz phase relations.—An attempt has been made to calibrate T–X(Fe–Mg) reactions at $PH_2O = 5$ kb (fig. 6) for the schematic diagrams presented in part I (figs. 1 and 2). The locations for the continuous reactions (3, involving Crd + Bio + Sil + Qtz with Mus or Ksp) are taken from figure 5. The location of the Mg end-member reactions 7 (Chl + Crd + Als), 1 (Chl + Bio + Als), and 16 (Chl + Crd + Bio) and in the Mus–Qtz field are taken from the data of Seifert (1970) and Bird and Fawcett (1973). The location of the Fe end-member reaction 12 (Sta + Gar + Sil) is taken from the data of Richardson (1968), and the location of K-Mus + Qtz = Ksp + Als + H_2O is taken from the data of Chatterjee and Johannes (1974). The location of the Mg-reactions 1 (Chl + Bio + Als) at 645°C and 16 (Chl + Crd + Bio) at 620°C for $PH_2O = 5$ kb implies that the discontinuous reaction (VIII, Chl + Mus = Bio + Crd + Sil) occurs between 620° to 645°C (see pt. I, fig. 1C). This temperature range limits the compositions of *Crd* ($X_{Mg} = 0.55$ to 0.65) and *Bio* ($X_{Mg} = 0.4$ to 0.5) involved in the continuous reaction (3, Mus + Crd = Bio + Sil + Qtz) in the interval 620° to 645°C at $PH_2O = 5$ kb (see fig. 6). The compositions of *Crd* and *Bio* involved in the continuous reactions (3, Crd + Bio + Sil) and (16, Chl + Crd + Bio) are identical at the discontinuous reaction (VIII, Chl + Mus = Bio + Crd + Sil). According to the construction in figure 6, the three-phase assemblage *Chl–Crd–Bio* in the AFM projection could move from the pure Mg side to the center of the diagram (such that $X_{Fe}^{Bio} = 0.5$ to 0.6) in this 25°C interval. The most iron rich compositions for this assemblage reported by Guidotti, Cheney, and Conatore (1975) are $X_{Fe}^{Bio} = 0.24$, $X_{Fe}^{Chl} = 0.22$, $X_{Fe}^{Crd} = 0.16$ which may imply a temperature increase of as little as 10°C for their observed movement of the three-phase triangle *Chl–Crd–Bio*. It is also impossible to distinguish the effects of a 10°C change in metamorphic temperature from gradients in fH_2O, which Guidotti, Cheney, and Conatore suggest caused the observed displacement.

In figure 6, the location of the discontinuous reaction (XVIII, Sta + Chl + Mus = Bio + Sil) is constrained (see pt. I, fig. 2) by the above location of discontinuous reaction (VIII) and the continuous reaction (1, Chl + Mus → Bio + Sil + Qtz) for which $T_{Mg} \approx 645$°C. The compositional ranges of coexisting *Sta + Bio + Chl* (solid rectangles at 610°C in fig. 6, from Guidotti, 1974) together with the above constraints suggest that discontinuous reaction (XVIII) lies only a few degrees below (VIII), at $PH_2O = 5$ kb. These discontinuous reactions would diverge at higher pressures (see fig. 7).

Discontinuous reaction (VII, Sta + Mus = Bio + Gar + Als) lies at higher temperatures than reaction 12 (Sta + Gar + Sil) in the pure Fe system where $T_{Fe} \approx 680$°C and below the K-Mus + Qtz = Ksp + Sil + H_2O reaction ($T \approx 695$°C at $PH_2O = 5$ kb). The continuous reaction loop 5 (Sta–Bio–Sil) is somewhat constrained by the compositions

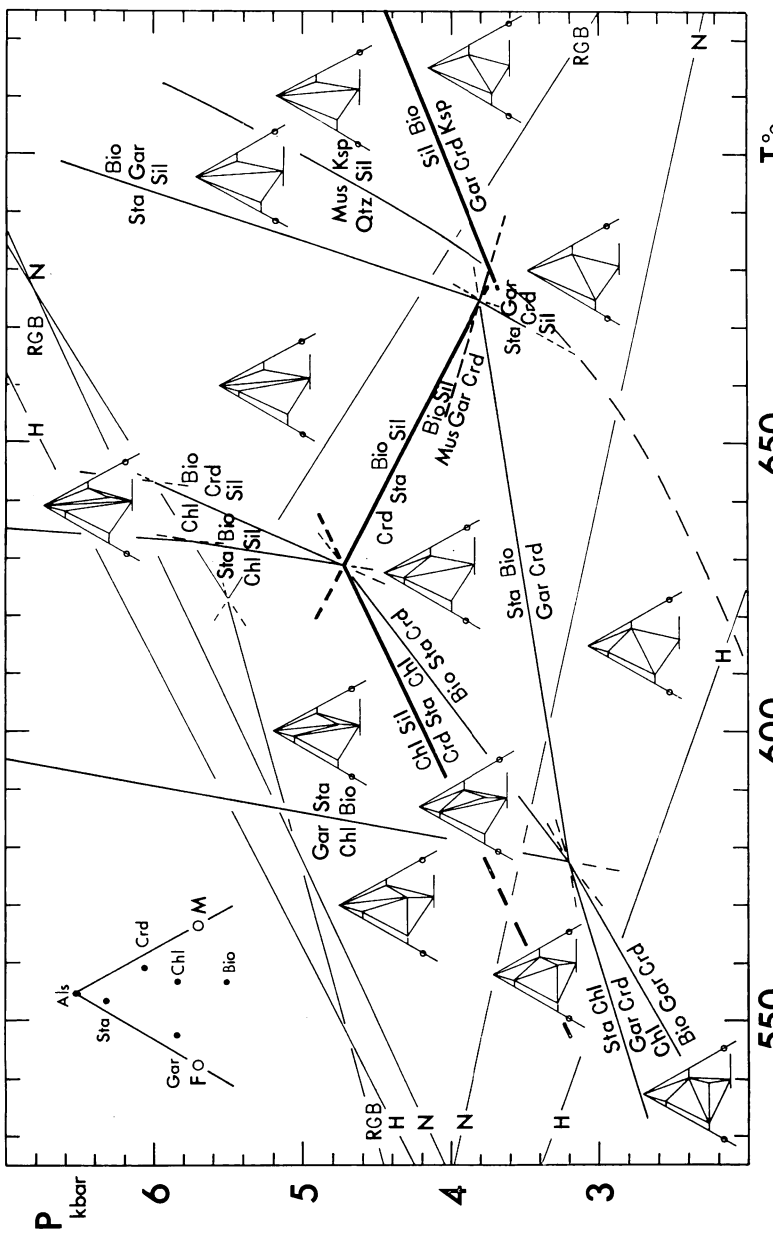

Fig. 7. Partial petrogenetic grid for discontinuous reactions in KFMASH (compare Hess, 1969, 1973). Reactions with chloritoid or hypersthene are not shown. Melting reactions and crystalline solution of Mn, Na, Ca, et cetera have been omitted. The Al_2SiO_5 relations of Newton (1966, *N*), Richardson, Gilbert, and Bell (1969, *RGB*), and Holdaway (1971, *H*) indicate that many of the discontinuous reactions occur in the region of uncertainty for the *And–Sil* equilibria. Inflections of discontinuous reactions involving *Als* have not been shown at any And–Sil boundary. The discontinuous reactions drawn with the heavy lines show the maximum pressure of cordierite occurrence in *most* common pelite compositions.

of this three-phase assemblage as reported by Guidotti (1970). The location of discontinuous reaction (XXXII, Gar + Chl + Mus = Sta + Bio) is least well constrained but may be located approximately by the positions of continuous reactions 23 (Gar + Sta + Bio, involved in discontinuous reaction VII) and 22 (Sta + Chl + Bio, involved in discontinuous reaction XVIII).

Comparison of calculated and observed phase relations in the staurolite to sillimanite transition.—Guidotti (1970, 1974) estimated pressures near 4 kb for the regional metamorphism in western Maine on the basis of Newton's (1966) location of the Al_2SiO_5 triple point. An analagous T–X(Fe–Mg) section calculated for $PH_2O = 4$ kb results in assemblages with higher X_{Fe} than indicated by the data of Guidotti. The correspondence of the compositions of the phases with a 5 kb isobaric T–X (Fe–Mg) section is considered to be due to the effect of Mn on the (Fe–Mg) continuous reactions (see Guidotti, 1974, p. 486) rather than to a higher pressure location of the Al_2SiO_5 triple point. The present calculations refer only to Fe–Mg continuous reactions, and Mn will displace the continuous reactions as functions of temperature and pressure in the manner discussed in part I (see also Dahl, 1968; Weisbrod, 1973b; Tracy, Robinson, and Thompson, in press).

It is significant to note that the assemblage *Sta–Gar–Sil* was not observed by Guidotti. This assemblage could be observed only if rocks of the appropriate Fe/Mg ratio and alumina content were present. The P–T location of Richardson's (1968) curve for the pure Fe-reaction 7 (Sta + Qtz = Gar + Sil + H_2O) suggests that the continuous reaction 7 (Sta + Gar + Sil) does not occur until just below the discontinuous reaction (VIII) and thus sets a lower temperature limit for this assemblage *in the Mn-free system.*

The experimental data of Hoschek (1969) provide further constraints on the location of two continuous reactions. For $X_{Fe} = 0.6$ at $PH_2O = 5$ kb, the solid triangle at 660°C (fig. 6) represents a maximum temperature for the divariant reaction 5 (Sta + Mus → Bio + Sil), and the open triangle at 580°C represents a maximum temperature for the divariant reaction 22 (Chl + Mus → Sta + Bio).

DISCONTINUOUS REACTIONS AND PETROGENETIC GRIDS

The discontinuous reactions in the KFMASH system may be located in P H_2O-T space because they originate (or terminate) at the specific invariant points (stable or metastable) in the (Fe–Mg) end-member systems KFASH and KMASH. Discontinuous reactions are the most suitable upon which to base petrogenetic grids, because they will result in easily observable mineralogical changes in pelitic rocks of a wide range of compositions (J. B. Thompson, 1957, p. 856). Grids constructed on the basis of (Fe–Mg) discontinuous reactions have been presented by Albee (1965), Hess (1969, 1973), Hoschek (1969), and Grant (1973).

The discontinuous reactions located in the present study result in a grid (fig. 7) that compares well with that of Hess except in the specific positions of some discontinuous reactions particularly those involved in the invariant point (Ch,H of Hess; relating *Sta–Gar–Bio–Crd–Als–Mus–Qtz*). One of these discontinuous reactions (III, *Sta* = *Crd* + *Crd* + *Als*) originates at the intersections of reactions 12 (*Sta* + *Qtz* → *Gar* + *Als*) and 10 (*Crd* → *Gar* + *Als* + *Qtz*) in the pure Fe-system (near 3.5 kb and 675°C, Richardson, 1968). The discontinuous reaction (III) originates at this intersection despite the fact that it lies in the stability field of anthophyllite (see Grieve and Fawcett, 1974, p. 134) and moves to higher pressure and temperature with increasing X_{Mg} (see figs. 6 and 7). This implies that the invariant point (Ch,H of Hess) occurs at higher pressures than 3.5 kb and temperatures than 670°C, see figure 7.

Some consequences of this location of the (Fe–Mg) invariant point (*Sta–Gar–Bio–Crd–Als–Mus–Qtz*) are not easily reconciled with natural observations. The observed assemblages *And–Gar–Bio* and *And–Gar–Crd* (with *Mus, Qtz,* see for example Osberg, 1971) would only have minor fields of stability with reference to the *And–Sil* transition of Richardson, Gilbert, and Bell (1969) and no field of stability with reference to the *And–Sil* transition of Newton (1966) or Holdaway (1971). These natural assemblages may be stabilized to lower pressures by the extensive crystalline solution of Mn (and smaller amounts of Ca) in natural garnet. It should be noted that Hess' (1969, 1973) grid was constructed on the basis of observed assemblages, while the present data (fig. 7) refer to only the K_2O–FeO–MgO–Al_2O_3–SiO_2–H_2O (KFMASH) system.

A further consequence of the location of the invariant point (Ch,H of Hess) at higher pressures and temperatures is the location of the discontinuous reaction (VII, *Sta* + *Mus* = *Bio* + *Gar* + *Als*) closer to the breakdown of *K-Mus* + *Qtz* to *Ksp* + *Als*. In a natural assemblage, sodic muscovite could react with plagioclase plus quartz at an even lower temperature than in the Ca–Na free system (see Thompson, 1974a). This would result in the appearance of *Sta–Ksp* according to the KFMASH system (+CaO and Na_2O) which apparently does not occur in natural assemblages (as noted by Hess, 1969, p. 196). Similarly, the commonly observed natural assemblage *Sil–Gar–Bio–Mus–Qtz* should not occur if figure 7 applied to all natural assemblages. In addition to displacement of continuous and discontinuous (Fe–Mg) reactions by Mn and reduced aH_2O (as discussed above), those reactions involving *Mus* and plagioclase will be displaced in natural assemblages containing Na_2O and CaO.

Even if the precise location of continuous and discontinuous reactions could be determined for the KFMASH system, significant differences would result between the experimentally and naturally observed assemblages. The above examples provide a caution in the assignment of "stable and unstable assemblages" in compositionally simple experimental systems on the basis of observed natural assemblages. It is clear that it will be impossible to construct a unique petrogenetic grid to which

all observed assemblages and reactions may be assigned. Nevertheless, grids based upon discontinuous reactions provide a more precise interpretation of metamorphic assemblages than any studies using end-member or even continuous reactions, alone.

APPLICATIONS, LIMITATIONS AND DEVELOPMENTS

The ability to predict, interrelate, and describe the behavior of a particular rock composition during metamorphism has attracted many novel ways of integrating experimental and thermochemical data with petrographic observation (for example, Carmichael, 1969; Brown and Skinner, 1974). The methods outlined here for predicting changes in AFM topology through P–X, T–X, and P–T sections give an instructive means of understanding the metamorphic development of specific assemblages and textures. The principal limitations to the present methods include uncertainties in the locations of Fe- and Mg-end member curves and in the estimated entropy values. Many of the relevant end-member reactions have not been investigated experimentally despite their obvious importance for location of continuous reactions. In many cases, either one or both Fe- and Mg-end member reactions may not be stable or the continuous reaction may only be stable over a small P–T range. The methods presented here may be used to guide experimental studies and focus on the key reactions.

Further limitations to the direct application of calculated KFMASH phase relations to natural assemblages include the unpredicted effects of additional components in natural crystalline solution and uncertainties as to the compositions of the equilibrium fluid phase. The general effects of Mn have been outlined above, and the effects of additional components upon natural reactions may be predicted from a knowledge of the relative solubility of such components in crystalline, melt, and fluid phases. The effects of Na on KASH phase relations have been considered by several workers (see above), and these may be combined with the predicted relations in KFMASH (compare Grant, 1973). Biotite reactions involving Na are displaced in the same way as those involving muscovite, alkali feldspar, and plagioclase. These relations may be quantified using analagous procedures as for muscovite–paragonite–feldspar–Al_2SiO_5 phase relations (compare Thompson, 1974a, fig. 2; and Rutherford, 1969, figs. 7 and 8).

The fact that the treatment of Fe-bearing systems in this study has not been concerned with oxidation reactions does not limit its application (see Fisher, 1965), if the amount of Fe^{3+} in biotite is small. If sufficient phases are present in a natural assemblage then reactions can be written independently of oxygen or hydrogen. Moreover, in most pelitic rocks fH_2O is generally several orders of magnitude greater than fO_2 or fH_2.

Mechanisms of metamorphic reactions.—Textural interpretation through reactions involving metasomatic cation exchange (see Chinner,

1962, p. 326; Carmichael, 1969; Fisher, 1970) may be considered a step further toward detailed petrographic interpretation than the methods outlined here. However, writing ionic reactions on the basis of textural relations alone may overlook significant compositional information, because ionic reactions may be operating differently in adjacent "local" systems. Moreover, some textures may indicate reactions that are locally unrelated to one another, because any polymetamorphic rock will usually record events over a range of P, T, and aH_2O.

The commonly observed overgrowth (or intergrowth in three dimensions!) of sillimanite on biotite (Chinner, 1961; Carmichael, 1969, p. 252) may simply be related to continuous reactions producing *Bio* + *Sil* from *Mus* + AFM phase (for example *Sta*), see also Thompson and Norton (1968, p. 323). Many of the textures described by Carmichael may be related to the appropriate continuous reactions shown in figure 5, above, and figure 2 in part I.

The methods using local metasomatic ionic reactions do, however, give important indications of the details of possible mechanisms and controls of particular reactions, which are not necessarily obvious from the P–T–X models described here. The methods of continuous reactions involving crystalline solutions may be developed for reactions involving ionic species in aqueous fluids, phases in equilibrium with anatectic melts, or reactions involving oxidation or reduction.

Estimation of metamorphic conditions using P–T–X(Fe–Mg) relations.—Extremely detailed petrography combined with careful chemical analysis is needed to define a facies type (specifying a particular limited range in P, T, and aH_2O) and to understand the development of specific textures in polymetamorphic rocks (see Chinner, 1962, p. 326, 333). Such observations in natural assemblages will lead to further refinements of the predicted displacements of mineral reactions due to additional components in crystalline solution and in the equilibrium fluid.

It is significant that P–T petrogenetic grids of the type shown in figure 7 are characterized by regions of closely-spaced discontinuous reactions and regions where certain facies types persist over wide P–T ranges. The most evident changes in natural assemblages will be those due to discontinuous reactions, and it is therefore not surprising that facies series from different regional metamorphic terrains show similar series of facies types (see Miyashiro, 1961; Albee, 1965b; Hietanen, 1967; Hess, 1969). The fact that chlorite, biotite, and garnet isograds (by whatever reaction!) in Barrovian-type facies series are often widely spaced and that staurolite, kyanite, and sillimanite isograds are often more closely spaced may be related to the relative positions of appropriate discontinuous reactions on petrogenetic grids rather than to complex geometrical arrangements between the deformed rock succession, isogradic surfaces, and geothermal gradients.

Use of the occurrences of the various Al_2SiO_5 polymorphs to identify precise pressures of metamorphism is particularly inaccurate for anda-

lusite–sillimanite type facies series. Many of the commonly observed discontinuous reactions probably occur within the region of uncertainty of location of the *And–Sil* boundary from different experimental investigations (see fig. 7). The specifications of complete facies types provide better estimates of metamorphic pressures than stability of individual Al_2SiO_5 polymorphs.

If the activity-composition relationships and appropriate continuous and discontinuous reactions between the minerals in pelitic rocks were known, the use of petrogenetic grids still suffers from uncertainty of knowledge of aH_2O during metamorphism. The P H_2O–T displacements of mineral reactions due to reduced aH_2O through chemical dilution by other components or to physical lowering due to "osmotic or fissure" equilibrium (J. B. Thompson, 1955) may be predicted. However, displacements of reactions on petrogenetic grids due to crystalline solution are not easily distinguished from the effect of reduced aH_2O.

Graphical analysis and analytical formulations of equilibrium relations.—Graphical analysis on the AKFM projection or P–X, T–X, and P–T sections becomes impractical for more than one significant "impurity" in the mineral phases. Analytical formulations (relations *viii, ix, x,* and *xi* above) for mineral equilibria, in terms of linear algebraic equations, may be modified simultaneously for crystalline solutions and reduced aH_2O. Moreover, values of $\Delta\bar{S}°_r$ and $\Delta\bar{H}°_r$, obtained from fitting x $\ln fH_2O$ against $1/T_K$ for experimental data in pure systems, may be compared with entropy and enthalpy data for the individual phases obtained by calorimetric or other thermochemical measurement. If activity-composition relationships for natural crystalline solutions were available, then equilibrium equations may be simultaneously solved for fH_2O. These methods are essential for the calibration of continuous and discontinuous reactions on the basis of compositions of coexisting natural phases, because the composition of the equilibrium fluid phase (even if buffered by the mineral assemblage) will change with progressive variation in pressure or temperature.

Future developments.—The P–T–X(Fe–Mg) relations may easily be extended to include other mineral phases (notably chloritoid, oxides, and sulfides) and other components (notably Mn, Na, Ca, and Fe^{3+}). Continuous reactions involving these components may be easily formulated by the addition of further binary cation exchange reactions to phase relations in KFMASH. The P–X and T–X sections and corresponding P–T grids, presented above, are constructed with sparse data and oversimplified models and as such should only be regarded as a basis for future development. Necessary refinements require further experimental determination of key end-member reactions and exchange reactions, in addition to comprehensive mineral analyses for complete facies types (such as the work of Albee, 1965a, 1972; Guidotti, 1970; and Guidotti, Cheney, and Conatore, 1975). Comparison between experimentally calibrated continuous reactions and those calculated with the simple crystalline solu-

tion models (pt. I, table 1) will lead to refinements of activity-composition relations for both mixing and ordering contributions. The calibration of cation and anion exchange reactions provides a most useful and probably accurate means of extrapolation from simple to complex systems.

ACKNOWLEDGMENTS

In addition to those acknowledged in part I, the writer would like to thank Arden L. Albee, Charles V. Guidotti, Robert C. Newton, Robert J. Tracy, and Peter Robinson for providing unpublished data.

REFERENCES

Albee, A. L., 1965a, Phase equilibria in three assemblages of kyanite-zone pelitic schists, Lincoln Mountain Quadrangle, central Vermont: Jour. Petrology, v. 6, p. 247-301.

———— 1965b, A petrogenetic grid for the Fe-Mg silicates of pelitic schists: Am. Jour. Sci., v. 263, p. 512-536.

———— 1972, Metamorphism of pelitic schists: reaction relations of chloritoid and staurolite: Geol. Soc. America Bull., v. 83, p. 3249-3268.

Atherton, M. P., 1968, The variations in garnet, biotite and chlorite compositions in medium grade rocks from the Dalradian, Scotland, with particular reference to the zonation in garnet: Contr. Mineralogy Petrology, v. 18, p. 347-371.

Best, M. G., and Weiss, L. E., 1964, Mineralogical relations in some pelitic hornfelses from the southern Sierra Nevada, California: Am. Mineralogist, v. 49, p. 1240-1266.

Bird, G. W., and Fawcett, J. J., 1973, Stability relations of Mg–chlorite–muscovite and quartz between 5 and 10 kb water pressure: Jour. Petrology, v. 14, p. 415-428.

Brown, T. H., and Skinner, B. J., 1974, Theoretical prediction of equilibrium phase assemblages in multi-component systems: Am. Jour. Sci., v. 274, p. 961-986.

Burnham, C. W., Holloway, J. R., and Davis, N. F., 1969, Thermodynamic properties of water to 1000°C and 10,000 bars: Geol. Soc. America Spec. Paper 132, 96 p.

Carmichael, D. M., 1969, On the mechanism of prograde metamorphic reactions in quartz-bearing pelitic rocks: Contr. Mineralogy Petrology, v. 20, p. 244-267.

Chatterjee, N. D., and Johannes, W., 1974, Thermal stability and standard thermodynamic properties of synthetic $2M_1$-muscovite, $KAl_2[AlSi_3O_{10}(OH)_2]$: Contr. Mineralogy Petrology, v. 48, p. 89-114.

Chernosky, J. V., 1974, The upper stability of clinochlore at low pressure and the free energy of formation of Mg–cordierite: Am. Mineralogist, v. 59, p. 496-507.

Chinner, G. A., 1961, The origin of sillimanite in Glen Clova, Angus: Jour. Petrology, v. 2, p. 312-323.

———— 1962, Almandine in thermal aureoles: Jour. Petrology, v. 3, p. 316-340.

Currie, K. L., 1971, The reaction 3 cordierite = 2 garnet + 4 sillimanite + 5 quartz as a geological thermometer in the Opinicon Lake region, Ontario: Contr. Mineralogy Petrology, v. 33, p. 215-226.

———— 1974, A note on the calibration of the garnet-cordierite geothermometer and geobarometer: Contr. Mineralogy Petrology, v. 44, p. 35-44.

Dahl, O., 1968, Hydrothermal studies of garnet-mica equilibria in the system 3(FeO, MnO)–$2Al_2O_3$–$12SiO_2$–K_2O–H_2O: Geol. fören. Stockholm Förh., v. 90, p. 331-348.

Dasgupta, H. C., Seifert, F., and Schreyer, W., 1974, Stability of manganocordierite and related phase equilibria in part of the system MnO–Al_2O_3–SiO_2–H_2O: Contr. Mineralogy Petrology, v. 43, p. 275-294.

Dougan, T. W., 1974, Cordierite gneisses and associated lithologies of the Guri Area, northwest Guayana Shield, Venezuela: Contr. Mineralogy Petrology, v. 46, p. 169-188.

Fed'kin, V. V., 1972, Calculation of mineral equilibria in the system FeO–Al_2O_3–SiO_2–O_2: Internat. Geology Rev., v. 14, p. 692-706.

Ferry, J. M., 1976, Metamorphism of calcareous sediments in the Waterville-Vassalboro area, south-central Maine: Am. Jour. Sci., v. 276, in press.

Fisher, G. W., 1965, The effect of variable oxygen activity on isograd reactions in pelitic rocks: Carnegie Inst. Washington Year Book 63, p. 279-283.

———— 1970, The application of ionic equilibria to metamorphic differentiation: An example: Contr. Mineralogy Petrology, v. 29, p. 91-103.

Froese, E., 1973, The oxidation of almandine and iron cordierite: Canadian Mineralogist, v. 11, p. 991-1002.

Fyfe, W. S., Turner, F. J., and Verhoogen, J., 1958, Metamorphic reactions and metamorphic facies: Geol. Soc. America Mem. 73, 259 p.

Ganguly, J., 1968, Analysis of the stabilities of chloritoid and staurolite and some equilibria in the system FeO–Al_2O_3–SiO_2–H_2O–O_2: Am. Jour. Sci., v. 266, p. 277-298.

———— 1972, Staurolite stability and related parageneses: Theory, experiments, and applications: Jour. Petrology, v. 13, p. 335-365.

Goldman, D. S., and Albee, A. L., 1976, Correlation of Mg/Fe partitioning between garnet and biotite with O^{18}/O^{16} partitioning between quartz and magnetite: Am. Mineralogist, in press.

Gorbatschev, R., 1968, Distribution of elements between cordierite, biotite and garnet: Neues Jahrb. Mineralogie Abh., v. 110, p. 57-80.

Grant, J. A., 1973, Phase equilibria in high-grade metamorphism and partial melting of pelitic rocks: Am. Jour. Sci., v. 273, p. 289-317.

Green, T. H., and Vernon, R. H., 1974, Cordierite breakdown under high-pressure, hydrous conditions: Contr. Mineralogy Petrology, v. 46, p. 215-226.

Greenwood, H. J., 1975, Thermodynamically valid projections of extensive phase relationships: Am. Mineralogist, v. 60, p. 1-8.

Grieve, R. A. F., and Fawcett, J. J., 1974, The stability of chloritoid below 10 kb PH_2O: Jour. Petrology, v. 15, p. 113-139.

Guidotti, C. V., 1970, The mineralogy and petrology of the transition from the lower to upper sillimanite zone in the Oquossoc Area, Maine: Jour. Petrology, v. 11, p. 277-336.

———— 1974, Transition from staurolite to sillimanite zone, Rangeley Quadrangle, Maine: Geol. Soc. America Bull., v. 85, p. 475-490.

Guidotti, C. V., Cheney, J. T., and Conatore, P., 1975, Coexisting cordierite + biotite + chlorite from the Rumford Quadrangle, Maine: Geology, v. 3, p. 147-148.

Hensen, B. J., 1971, Theoretical phase relations involving cordierite and garnet in the system MgO–FeO–Al_2O_3–SiO_2: Contr. Mineralogy Petrology, v. 33, p. 191-214.

———— 1973, Cordierite–garnet equilibrium as a function of pressure, temperature, and iron-magnesium ratio: Carnegie Inst. Washington Year Book 72, p. 418-425.

Hensen, B. J., and Green, D. H., 1971, Experimental study of the stability of cordierite and garnet in pelitic compositions at high pressures and temperatures. I. Compositions with excess alumino-silicate: Contr. Mineralogy Petrology, v. 33, p. 309-330.

———— 1972, II. Compositions without excess-aluminosilicate: Contr. Mineralogy Petrology, v. 35, p. 331-354.

———— 1973, III. Synthesis of experimental data and geological applications: Contr. Mineralogy Petrology, v. 38, p. 151-166.

Hess, P. C., 1969, The metamorphic paragenesis of cordierite in pelitic rocks: Contr. Mineralogy Petrology, v. 24, p. 191-207.

———— 1971, Prograde and retrograde equilibria in garnet–cordierite gneisses in south-central Massachusetts: Contr. Mineralogy Petrology, v. 30, p. 177-195.

———— 1973, Figure 9, *in* Miyashiro, Akiho, Metamorphism and Metamorphic Belts: New York, Halsted Press, p. 81.

Hietanen, A., 1967, On the facies series in various types of metamorphism: Jour. Geology, v. 75, p. 187-214.

Hirschberg, A., and Winkler, H. G. F., 1968, Stabilitatsbeziehungen zwischen Chlorit, Cordierit und Almandin bei der Metamorphose: Beitr. Mineralogie Petrographie, v. 18, p. 17-42.

Holdaway, M. J., 1971, Stability of andalusite and the aluminum silicate phase diagram: Am. Jour. Sci., v. 271, p. 97-131.

Hoschek, G., 1969, The stability of staurolite and chloritoid and their significance in metamorphism of pelitic rocks: Contr. Mineralogy Petrology, v. 22, p. 208-232.

Hsu, L. C., 1968, Selected phase relationships in the system Al–Mn–Fe–Si–O–H. A model for garnet equilibria: Jour. Petrology, v. 9, p. 40-83.

Hutcheon, I., Froese, E., and Gordon, T. M., 1974, The assemblage quartz–sillimanite–garnet–cordierite as an indicator of metamorphic conditions in the Daly Bay Complex, N.W.T.: Contr. Mineralogy Petrology, v. 44, p. 29-34.

Kleppa, O. J., and Newton, R. C., in press, The role of solution calorimetry in the study of mineral equilibria: Fortschr. Mineralogie, in press.

Korzhinskii, D. S., 1959, Physicochemical basis of the analysis of the parageneses of minerals: New York, Consultants Bur., 142 p.

Kretz, Ralph, 1961, Some applications of thermodynamics to coexisting minerals of variable composition: Jour. Geology, v. 69, p. 361-387.

———— 1972, Theory of chemical exchange reactions in crystalline rocks: Internat. Geol. Cong., Montreal, Canada 1972, Proc., v. 10, p. 67-77.

Latimer, W. M., 1951, Methods of estimating the entropy of solid compounds: Am. Chem. Soc. Jour., v. 73, p. 1480-1492.

Lyons, J. B., and Morse, S. A., 1970, Mg/Fe partitioning in garnet and biotite from some granitic, pelitic and calcic rocks: Am. Mineralogist, v. 55, p. 231-245.

Miyashiro, Akiho, 1961, Evolution of metamorphic belts: Jour. Petrology, v. 2, p. 277-311.

Mueller, R. F., 1961, Analysis of relations among Mg, Fe, and Mn in certain metamorphic minerals: Geochim. et Cosmochim. Acta, v. 25, p. 267-296.

Newton, R. C., 1966, Kyanite–andalusite equilibrium from 700° to 800°C: Science, v. 153, p. 170-172.

———— 1972, An experimental determination of the high-pressure stability limits of magnesian cordierite under wet and dry conditions: Jour. Geology, v. 80, p. 398-420.

Newton, R. C., Charlu, T. V., and Kleppa, O. J., 1974, A calorimetric investigation of the stability of anhydrous magnesium cordierite with application to granulite facies metamorphism: Contr. Mineralogy Petrology, v. 44, p. 295-311.

Okrusch, M., 1971, Garnet–cordierite–biotite equilibria in the Steinach Aureole, Bavaria: Contr. Mineralogy Petrology, v. 32, p. 1-23.

Osberg, P. H., 1971, An equilibrium model for Buchan-type metamorphic rocks, south-central Maine: Am. Mineralogist, v. 56, p. 569-576.

Reinhardt, E. W., 1968, Phase relations in cordierite-bearing gneisses from the Gananoque area, Ontario: Canadian Jour. Earth Sci., v. 5, p. 455-482.

Richardson, S. M., ms, 1975, Application of retrograde cation-exchange profiles to metamorphic cooling rates: Ph.D. thesis, Harvard Univ.

Richardson, S. W., 1968, Staurolite stability in a part of the system Fe–Al–Si–O–H: Jour. Petrology, v. 9, p. 467-488.

Richardson, S. W., Gilbert, M. C., and Bell, P. M., 1969, Experimental determination of kyanite–anadalusite and anadalusite–sillimanite equilibria; the aluminum silicate triple point: Am. Jour. Sci., v. 267, p. 259-272.

Robie, R. A., 1965, Heat and free energy of formation of herzenbergite, troilite, magnesite and rhodochrosite calculated from equilibrium data: U.S. Geol. Survey Prof. Paper 525-D, p. 65072.

Robie, R. A., Bethke, P. M., and Beardsley, K. M., 1967, Selected X-ray crystallographic data, molar volumes, and densities of minerals and related substances: U.S. Geol. Survey Bull. 1248, 87 p.

Rutherford, M. J., 1969, An experimental determination of iron biotite-alkali feldspar equilibria: Jour. Petrology, v. 10, p. 381-409.

Rutherford, M. J., and Eugster, H. P., 1967, Experimental determination of the stability of aluminous biotite [abs.]: Canadian Mineralogist, v. 9, p. 305-306.

Saxena, S. K., 1969, Silicate solid solutions and geothermometry 3. Distribution of Fe and Mg between coexisting garnet and biotite: Contr. Mineralogy Petrology, v. 22, p. 259-267.

Schreyer, W., and Seifert, F., 1969, Compatibility relations of the aluminum silicates in the systems $MgO–Al_2O_3–SiO_2–H_2O$ and $K_2O–MgO–Al_2O_3–SiO_2–H_2O$ at high pressures: Am. Jour. Sci., v. 267, p. 371-388.

Seifert, F., 1970, Low-temperature compatibility relations of cordierite in heplopelites of the system $K_2O–MgO–Al_2O_3–SiO_2–H_2O$: Jour. Petrology, v. 11, p. 73-99.

Seifert, F., and Schreyer, W., 1970, Lower temperature stability limit of Mg cordierite in the range 1-7 kb water pressure: A redetermination: Contr. Mineralogy Petrology, v. 27, p. 225-238.

Stout, J. H., 1975, Apparent effects of molecular water on the lattice geometry of cordierite: Am. Mineralogist, v. 60, p. 229-234.

Thompson, A. B., 1974a, Calculation of muscovite–paragonite–alkali feldspar phase relations: Contr. Mineralogy Petrology, v. 44, p. 173-194.

———— 1974b, Gibbs energy of aluminous minerals: Contr. Mineralogy Petrology, v. 48, p. 123-126.

Thompson, J. B., Jr., 1955, The thermodynamic basis for the mineral facies concept: Am. Jour. Sci., v. 253, p. 65-103.

———— 1957, The graphical analysis of mineral assemblages in pelitic schists: Am. Mineralogist, v. 42, p. 842-858.

Thompson, J. B., Jr., and Norton, S. A., 1968, Paleozoic regional metamorphism in New England and adjacent areas, *in* Zen, E-an, Studies of Appalachian Geology: Northern and Maritime: New York, Intersci., p. 319-327.

Tracy, R. J., ms, 1975, High grade metamorphic reactions and partial melting in pelitic schist, Quabbin Reservoir Area, Massachusetts: Ph.D. thesis, Univ. Mass., Amherst, 127 p.

Tracy, R. J., Robinson, P. R., and Thompson, A. B., in press, Garnet composition and zoning in the determination of temperature and pressure of metamorphism, central Massachusetts: Am. Mineralogist, in press.

Weisbrod, A., 1973a, Refinements of the equilibrium conditions of the reaction Fe cordierite → almandine + quartz + sillimanite (+H O): Carnegie Inst. Washington Year Book 72, p. 518-521.

———— 1973b, Cordierite–garnet equilibrium in the system Fe–Mn–Al–Si–O–: Carnegie Inst. Washington Year Book 72, p. 515-518.

Zen, E-an, 1973, Thermochemical parameters of minerals from oxygen-buffered hydrothermal equilibrium data: method, application to annite and almandine: Contr. Mineralogy Petrology, v. 39, p. 65-80.